Dyes and Pigments 163 (2019) 667–674

Contents lists available at ScienceDirect

Dyes and Pigments

journal homepage: www.elsevier.com/locate/dyepig

A colorimetric and fluorometric oligothiophene-indenedione-based sensor for rapid and highly sensitive detection of cyanide in real samples and bioimaging in living cells

Zongrang Guo, Tingting Hu, Tao Sun, Tianduo Li*, Hong Chi, Qingfen Niu**

Shandong Provincial Key Laboratory of Molecular Engineering, School of Chemistry and Pharmaceutical Engineering, Qilu University of Technology (Shandong Academy of Sciences), Jinan, 250353, People's Republic of China

ARTICLE INFO

Keywords:
Oligothiophene-indenedione
Colorimetric sensor
Fluorometric sensor
Cyanide
Real sample
Live-cell imaging

ABSTRACT

A new simple oligothiophene-indenedione-based sensor **3TI** has been synthesized for the highly reactive and selective detection of cyanide anion (CN^-) in 70% aqueous media. The sensor **3TI** displays distinct colorimetric and fluorometric detection of CN^- due to the addition of CN^- to the electron-deficient indenedione-vinyl group of **3TI**, which hampers intramolecular charge transfer (ICT) efficiencies. The recognition mechanism of **3TI** for CN^- was confirmed by the optical measurements, ^1H NMR titration, FTIR spectra, HRMS analysis, and TD-DFT calculations. The sensor **3TI** for CN^- shows the outstanding advantages of high fluorescence brightness, fast response time (30 s), low detection limit (31.3 nM), minimal pH dependence in the physiologically relevant range, and excellent selectivity in presence of other competitive anions. Encouraged by these desirable sensing properties, the **3TI** has been successfully used for determination of CN^- in real water and food samples, silica-based sensing kits and fluorescence imaging in living cells with satisfactory results.

1. Introduction

Cyanide (CN^-) is well-known for its extreme toxicity to mammals because of its ability to bind to the active site of cytochrome oxidase and inhibit cellular respiration [1]. CN^- poisoning can result in vomiting, convulsions, unconsciousness, and eventual death. Nevertheless, cyanide as an important chemical reagent is extensively used in diverse areas such as electroplating, metal mining, plastic manufacture and X-ray film recovery, and can easily reach the environment [2]. In addition, in nature cyanide generally occurs in many food and plants, such as cassava, bamboo shoots, sorghum, green potatoes, sprouting potatoes, and bitter seeds [3]. As a result, the widespread application of CN^- anions raises a large number of environmental concerns, particularly in terms of its retention in leech circuits, recovery, and potential for contamination [4]. Only 0.5–3.5 mg of cyanide per kilogram of body weight can lead to death in humans [5,6]. The World Health Organization (WHO) allows the maximum acceptable level of CN^- in drinking water less than 1.9 μM [7]. Despite safeguards and stringent norms set by different regulatory bodies, the any accidental release of cyanide to the environment can contaminate drinking water and cause serious problems. All the above factors extremely need the development of an efficient method for detecting CN^- in aqueous as well as in cellular environments. Traditional detection methods (such as potentiometry and conventional titration) are expensive, laborious, time consuming, and require complicated instrumentation and skillful operators, which greatly limited their wide applications. Therefore, these limitations leave distinct scope for the development of a safe, simple, selective and sensitive molecular sensor for CN^- detection and quantification in environmental and biological systems.

A number of excellent sensors have been developed in recent years [8,9], however, colorimetric and fluorometric sensors for CN^- anions have received considerable attention due to their outstanding features such as their user-friendly nature suitable for on-site analysis, simplicity, high sensitivity and selectivity, visual detection, and potential for in vivo imaging [10–14]. Simultaneously, colorimetric sensing, which allows convenient monitoring of target CN^- anions by the naked eye without resorting to any expensive instrumentation, has appealed great attention in recent years [15–17]. The design of CN^--selective fluorescent sensors generally relies on the nucleophilic attack of CN^- on the electrophilic functional group such as dicyanovinyl [18–23], aldehyde [24–27], indolium [28–31], barbituric acid [32] and trifluoromethyl group [33], resulting in changes in π-conjugated system and thus the

* Corresponding author.
** Corresponding author.
E-mail addresses: litianduo@163.com (T. Li), qf_niu1216@qlu.edu.cn (Q. Niu).

https://doi.org/10.1016/j.dyepig.2018.12.057
Received 7 November 2018; Received in revised form 10 December 2018; Accepted 25 December 2018
Available online 28 December 2018
0143-7208/

special fluorescent properties. This exhibits high sensitivity and excellent selectivity for CN^- detection. However, some of them also show several drawbacks such as narrow pH working range, lack of sensing ability in aqueous solution, inability to perform cellular imaging, lack of colorimetric change and creation of turn-off instead of turn-on fluorescent sensor. Therefore, developing a new colorimetric and turn-on fluorescent sensor for CN^- detection with favorable working pH span, high sensitivity and cell-penetrating ability would be highly desirable.

In view of this requirement and as part of our research effort devoted to ion recognition, herein, we have designed and synthesized a new simple oligothiophene-indenedione-based colorimetric and turn-on fluorescent sensor for the naked-eye detection of CN^- in THF/H_2O (3:7, v/v) solution based on the mechanism of intramolecular charge transfer (ICT) inhibiting. What's more, this sensor features a lot of benefits, such as colorimetric and turn-on fluorescence dual-mode response, high selectivity and sensitivity, fast response time, favorable working pH range, and applicability in physiological conditions. The sensor could detect cyanide in real water and food samples as well as the silica based sensing kits. In addition, the novel sensor is well biocompatible, which is an added advantage for living cells applications.

2. Experimental section

2.1. Materials and instrumentations

All chemical reagents and solvents used were obtained commercially at analytical grade and used without further purification. Deionized water was used throughout the experiment. Tetrabutylammonium salt of anions (CN^-, F^-, Cl^-, AcO^-, NO_3^-, SCN^-, CO_3^{2-}, HCO_3^-, HS^-, HSO_3^-, HSO_4^- and SO_4^{2-}) were purchased from Sigma-Aldrich and stored in vacuum desiccators. The various anions above were diluted to 1.0×10^{-3} M by deionized water to obtain the stock solutions. The deionized water obtained from the Millipore Milli-Q system with 18 MΩ was used throughout all of the experiments. All the analytical solutions were prepared in THF/H_2O (3:7, v/v) solution. Compounds **3T** and **3T-CHO** were prepared according to the well-known literature procedure [34].

NMR spectra were recorded on Bruker AvanceII NMR spectrometer at an operating frequency of 400 MHz for ^1H NMR and 100 MHz for ^{13}C NMR in DMSO-d_6. Infrared spectra of **3TI** and **3TI-CN**$^-$ were recorded on Bruker ALPHA FT-IR spectrometer using KBr pellets. High-resolution mass spectra (HRMS) were recorded on Agilent 6510 Accurate-Mass Q-TOF LC/MS system. The UV–Vis absorption and emission spectra were measured using a Shimadzu UV-2600 and Hitachi F-4600 fluorescence spectrophotometer, respectively. The fluorescence images were collected by a Leica TCS SP8 confocal-laser scanning microscope (CLSM) with an objective oil lens of 63X magnification. All pH measurements were performed with a PHS-3C meter.

2.2. Synthesis of sensor *3TI*

Compound **3T-CHO** (100 mg, 0.36 mmol) and 1,3-indendione (52.9 mg, 0.36 mmol) were dissolved in dry EtOH (50 mL). The mixture was stirred under reflux overnight. Then the mixture was cooled to room temperature, and the formed precipitate was filtered off, washed with ethanol and dried in vacuum to obtain pure compound **3TI** (130.3 mg, yield 89%)as a deep red solid. ^1H NMR: (400 MHz, DMSO-d_6, ppm): δ = 8.22 (d, J = 4.0 Hz, 1H), 8.07 (s, 1H), 7.93–7.97 (m, 4H), 7.65–7.68 (m, 2H), 7.64 (d, J = 8.0 Hz, 1H), 7.49 (d, J = 4.0 Hz, 1H), 7.44 (d, J = 4.0 Hz, 1H), 7.16 (t, J = 4.0 Hz, 1H); ^{13}C NMR: (100 MHz, DMSO-d_6, ppm): δ = 189.28, 189.10, 148.37, 145.48, 141.33, 139.90, 138.70, 135.56, 135.52, 135.44, 135.41, 135.28, 133.98, 128.63, 128.22, 126.70, 125.60, 125.49, 125.24, 123.32, 122.70, 122.56; HRMS (ESI): m/z $[M+H]^+$ calcd for: $C_{22}H_{13}O_2S_3$: 405.0078, found: 405.0071; FTIR: (KBr, cm^{-1}) ν = 1721 (C=O), 1676 (C=C, 1,3-indenedione-vinyl), 1621, 1594 and 1573 (C=C, aromatic ring).

2.3. Theoretical calculation

All theoretical calculations were carried out by using the Gaussian 09 program package [35]. Geometries of the sensor **3TI** and its complex **3TI-CN**$^-$ were optimized by using density functional theory (DFT) calculations at the B3LYP/6-31G* level of theory [36,37], and then, the time-dependent density functional theory (TD-DFT) method was used to obtain the transition energy and absorption spectra. The binding pattern of **3TI** with CN^- were further proposed from the calculation results using DFT/TD-DFT method.

2.4. Cytotoxicity assay

The cytotoxicity of sensor **3TI** to HeLa cells was studied through a MTT assay. HeLa cells were seeded into 96-well microplates at a density of 1×10^5 cells/mL in 100 μL medium containing 10% FCS (Fetal Calf Serum) and incubated for 24 h. The cells were cultured in different concentrations (0–30 μM) of sensor **3TI** solutions in incubator (37 °C, 5% CO_2 and 95% air) for 24 h. After that, 10 μL MTT (5 mg/mL) was added to each well and continue incubated for another 4 h. Then, these cells were dissolved in DMSO (150 μL $well^{-1}$), and the absorbance level was analyzed at 492 nm by microplate reader (Multiskan™ FC Microplate Photometer, Thermo Scientific, USA). The treated wells relative to that in the control and the culture medium was used as a control.

2.5. Cell culture and fluorescence imaging

The living HeLa cells that were cultured in DMEM (Dulbecco's Modified Eagle's Medium) supplemented with 10% FBS (fetal bovine serum) at 37 °C under an atmosphere of 5% CO_2 were chosen for the cell imaging experiments. First, the living HeLa cells and sensor **3TI** (10 μM) were cultured in cell culture medium for 1 h at 37 °C, washed with PBS buffer (pH = 7.4) for three times, and then imaging. Then, cyanide ion (25 μM) was added to the pre-cultured cells of the sensor **3TI**, cultured for 30 min at 37 °C, washed with PBS buffer (pH = 7.4) for three times, then imaging. After 60 min, imaging the cells that loaded cyanide ion again were observed under CLSM. The fluorescence for **3TI** images were taken by excitation at 488 nm and the emission was collected from 500 to 550 nm.

3. Results and discussion

3.1. Preparation of *3TI*

The sensor **3TI** was successfully synthesized by a straightforward condensation reaction of compound **3T-CHO** with 1,3-indenedione in EtOH as the solvent to give the product in 89% yield as depicted in Scheme 1. The resultant product **3TI** was fully characterized by using standard spectroscopic techniques such as ^1H NMR, ^{13}C NMR, FTIR and HRMS spectra (Figs. S1–S4).

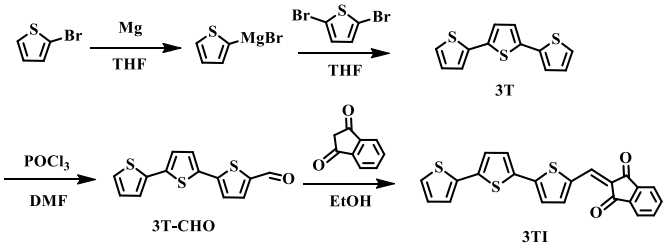

Scheme 1. The synthetic route of sensor **3TI**.

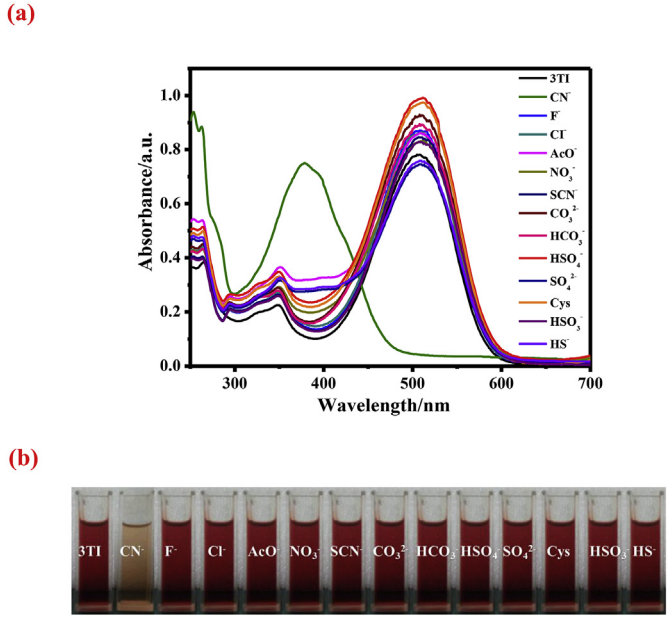

Fig. 1. (a) The UV–vis absorption spectra of sensor **3TI** (1.0 μM) towards 10.0 equiv. various analytes in THF/H_2O (3:7, v/v) solution; **(b)** Visual solution color change in **3TI** in the presence of various analytes in the sun light. (For interpretation of the references to color in this figure legend, the reader is referred to the Web version of this article.)

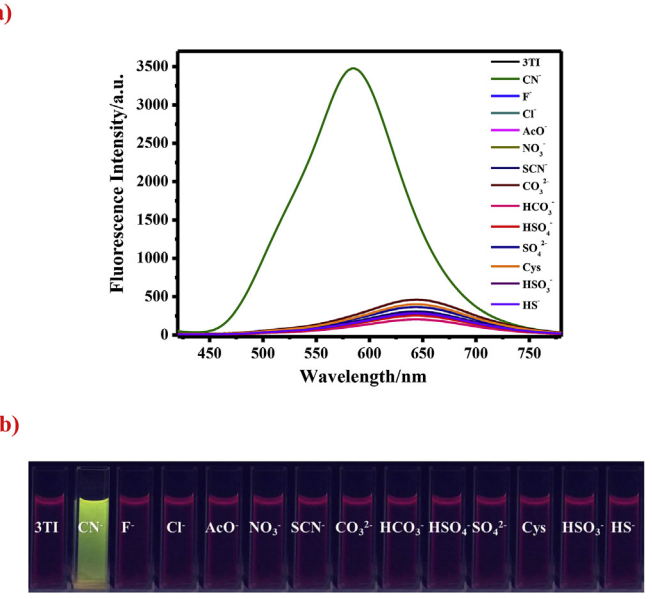

Fig. 2. (a) Changes in the emission spectra of **3TI** (1.0 μM) upon addition of different analytes (10.0 equiv.) in THF/H_2O (3:7, v/v) solution; **(b)** Fluorescence color changes upon different analytes added to sensor **3TI** under 365 nm UV lamp. (For interpretation of the references to color in this figure legend, the reader is referred to the Web version of this article.)

3.2. The optical response of sensor *3TI* toward CN^-

The sensing abilities of **3TI** were investigated by UV–Vis spectroscopy and fluorescence spectroscopy in THF/H_2O (3:7, v/v) solution. The UV–vis spectra of the **3TI** (1.0 μM) shows a low energy band at 512 nm and a high energy band at 349 nm due to intramolecular charge transfer (ICT) from oligothiophene moiety to electron deficient 1,3-indenedione moiety and π-π* transition, respectively. When different kinds of analytes (10 equiv.) such as CN^-, F^-, Cl^-, AcO^-, NO_3^-, SCN^-, CO_3^{2-}, HCO_3^-, HSO_4^-, SO_4^{2-}, HS^-, HSO_3^-, and cysteine (Cys) were respectively added to the solution of **3TI** (1.0 μM), only CN^- was found to result in a dramatic color change from red to colorless (Fig. 1a), which can be easily detected by the naked-eyes. In the corresponding UV–Vis spectra, the absorption band at 512 nm (ICT) completely disappeared and a new strong band at 378 nm appeared (Fig. 1b). These obvious changes indicate that the nucleophilic addition of CN^- to the electron deficient part of **3TI** results in inhibition of ICT transition. However, other tested analytes (F^-, Cl^-, AcO^-, NO_3^-, SCN^-, CO_3^{2-}, HCO_3^-, HSO_4^-, SO_4^{2-}, HS^-, HSO_3^- and Cys) induced almost no significant change in color and absorption spectra (Fig. 1b). These observations reveal that **3TI** can be used as a good colorimetric sensor for CN^- in aqueous media.

Fig. 2 shows the fluorescence response of sensor **3TI** toward CN^-. The free sensor **3TI** exhibited a very weak fluorescence emission band at 643 nm upon excitation at 390 nm in THF/H_2O (3:7, v/v) solution. The only significant response was observed when CN^- (10 equiv.) was added. A prominent fluorescent enhancement at 588 nm (37-fold) was clearly observed and the band at 643 nm (ICT) diminished, which responded with an obvious color change from red to bright green under UV lamp (Fig. 2b). This can be explained by that CN^- acted as a good nucleophile attacks to the electrophilic center of the **3TI** to suppress the π-conjugation resulting in distinct change in solution color and fluorescence. However, other examined analytes (10 equiv.) did not lead to any significant change in solution color and fluorescence spectra of **3TI**, demonstrating that **3TI** could effectively sense CN^- in aqueous solution with high selectivity.

3.3. Anti-interference capacity

Excellent anti-interference capacity is a key factor for a good CN^- fluorescent sensor. Thus, to validate anti-interference capability of sensor **3TI**, competitive experiments were performed in the presence of 10 equiv. of CN^- and 10 equiv. of various other tested analytes aforementioned by fluorescence spectroscopy (Fig. 3). These tested analytes except for CN^- gave no visible change and were not found to induce any significant interference even at higher concentrations. These findings confirmed the excellent selectivity and excellent anti-interference capacity of sensor **3TI** for CN^- against all kinds of analytes.

To get insight into the CN^- (1.0 μM) sensing property of sensor **3TI**, the fluorescence titration experiment was carried out with different concentrations of CN^- in THF/H_2O (3/7, v/v) solution. As shown in Fig. 4, upon gradual addition of CN^- (0–10 equiv.), a prominent fluorescent enhancement at 588 nm accompanied by a blue shift of

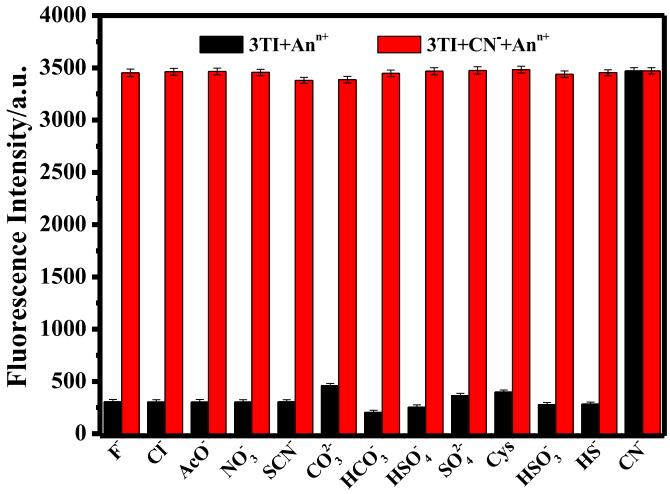

Fig. 3. Competitive experiments of **3TI** (1.0 μM) for CN^- (10.0 equiv.) in the presence of common analytes (10.0 equiv.) in THF/H_2O (3:7, v/v) solution. Excitation wavelength at 390 nm, emission wavelength at 588 nm.

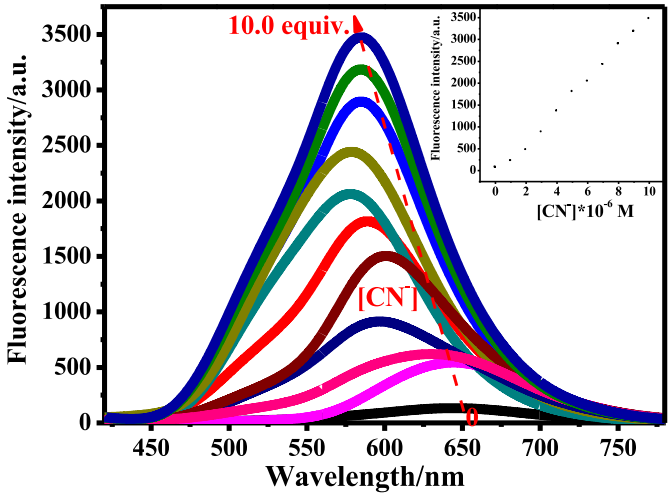

Fig. 4. Fluorescence titration of sensor **3TI** (1.0 μM) with the gradual increasing of concentrations of CN^- anions (0–10.0 equiv.). **Inset**: Fluorescence calibration curve at 588 nm of **3TI** as a function of the CN^-.

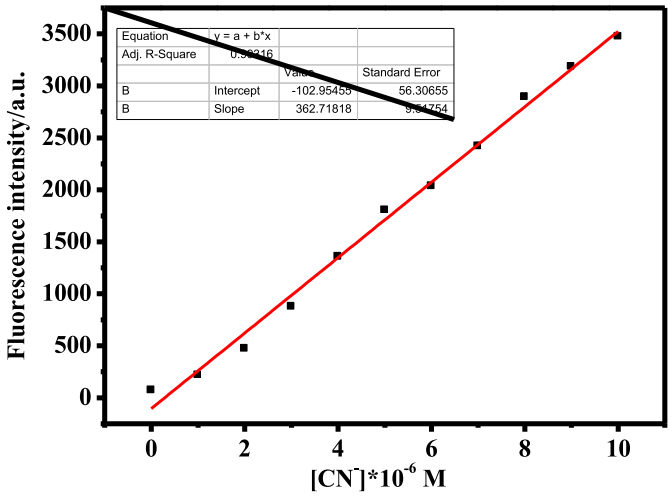

Fig. 5. The linear relationship between fluorescence intensity at 588 nm and the concentrations of CN^-.

55 nm from 643 to 588 nm, and the fluorescent intensity of sensor **3TI** at 588 nm gradually increased with the increased of CN^- (Fig. 4, inset), indicating that the ICT process was hampered by the nucleophilic attack of CN^- to the vinyl group of sensor **3TI**. The increase in emission intensity at 588 nm as a function of [CN^-] was found to be good linear for [CN^-] of 0–10 μM with regression coefficient of $R^2 = 0.99316$ (Fig. 5), suggesting the good fluorescent sensing ability of **3TI** for CN^- in aqueous media. The detection limit (DL) of **3TI** for CN^- by the fluorescence spectra changes was calculated to be 31.3 nM based on $3\delta/S$ [38,39], which is much lower than the WHO detection level (1.9 μM) [7] and the US EPA established the Maximum Contaminant Level (MCL) for CN^- in drinking water to be 2.0 μM [40]. Thus, these results indicated that sensor **3TI** can be used to detect low concentration of CN^- in practical application.

3.4. Sensing mechanism of sensor *3TI* toward CN^-

To get insight into the sensing mechanism of the sensor **3TI** to CN^-, the reaction product of **3TI** with CN^- was investigated by ^1H NMR and FTIR spectra. Fig. 6 shows the ^1H NMR spectra date before and after cyanide anion addition in DMSO-d_6 at room temperature. The addition of CN^- caused a slow reduction of the vinyl proton signal (H_K) at

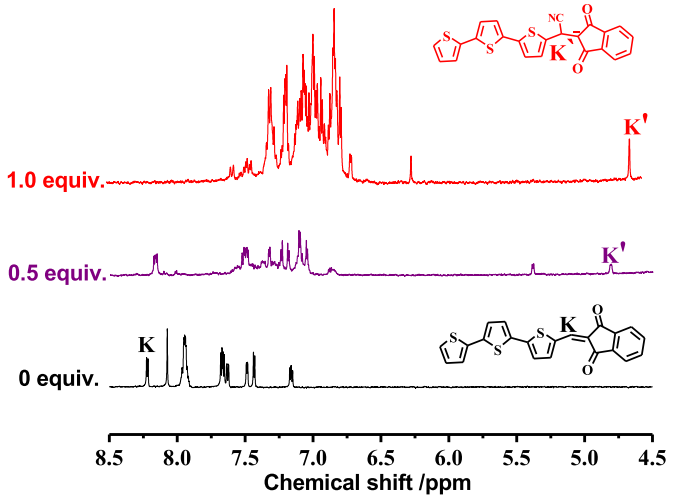

Fig. 6. ^1H NMR spectra (400 Hz, DMSO-d_6) of sensor **3TI** in the absence and presence of CN^- (0.5 equiv. and 1.0 equiv.).

8.22 ppm, which completely disappeared upon the addition of 1.0 equiv. of CN^-, while a new signal emerged at 4.85 ppm, which corresponds to the β-proton of 1,3-indenedione-vinyl group ($H_{K'}$). Meanwhile, the aromatic proton signals showed substantial upfield shifts compared to those of sensor **3TI** due to breaking of the conjugation. These results indicated that CN^- attacks the *β*-conjugated position of 1,3-indenedione-vinyl moiety of sensor **3TI** and the formation of cyanide adduct (**3TI**-CN^-). The interaction mechanism between **3TI** and CN^- was also supported by FTIR measurements (Fig. S5). In the presence of CN^- (1.0 equiv), it was clearly observed that the characteristic stretching band for the saturated hydrocarbon (CH) group appeared at 2956 and 2881 cm^{-1} and a new absorption peak at 2143 cm^{-1} observed corresponding to the C≡N group. Meanwhile, the C=C stretching frequency of the 1,3-indenedione-vinyl moiety at 1676 cm^{-1} completely disappeared and the stretching vibration absorption peak of amide (C=O) shifted from 1721 to 1687 cm^{-1}. These findings strongly proved that the coordination undergo the nucleophilic addition of CN^- to 1,3-indenedione-vinyl group. In addition, the formation of the corresponding **3TI-CN⁻** adduct was further confirmed by HR ESI-MS analysis (Fig. S6), where the peak at *m/z* 430.9075 (calc. = 431.0108) corresponding to [**3TI-CN⁻** + H]$^+$ was clearly observed, the signal at *m/z* = 449.0273 (*m/z* calcd. = 449.0214) corresponds to [**3TI-CN⁻** + H_2O]$^+$, and an obvious signal at *m/z* = 493.0505 appeared, coinciding exactly with that for the adduct species of [**3TI-CN⁻** + NO_3^-]$^+$ (*m/z* calcd. = 492.9987).

Based on these observations, the proposed sensing mechanism was the nucleophilic addition of CN^- to **3TI** (Scheme 2), which efficiently hampered the ICT process [41–43], and thus caused the solution dramatic naked-eye detectable color changes, large enhancement of emission and the optical spectral blue shift.

3.5. Theoretical calculations

To further gain insight into the sensing mechanism of the color bleaching and fluorescence off-on behavior of **3TI** in the presence of

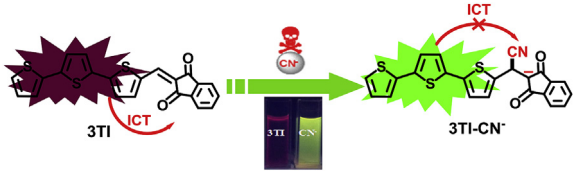

Scheme 2. The proposed mechanism of sensor **3TI** for CN^- detection.

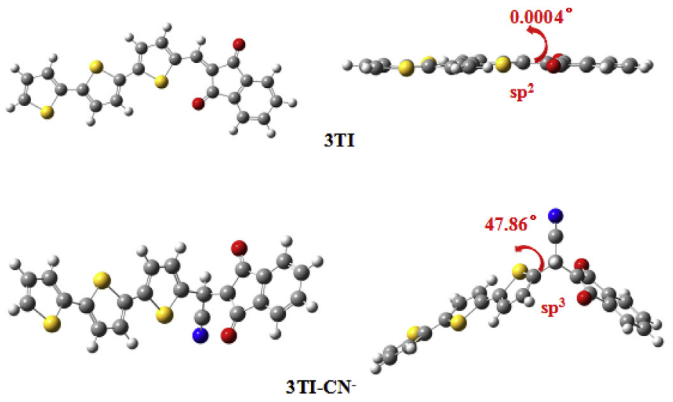

Fig. 7. Optimized structures of **3TI** and **3TI-CN⁻**.

CN^-, the computer calculations were carried out by B3LYP/6-31G* method. Fig. 7 shows the optimized geometries of **3TI** and **3TI-CN⁻**. Sensor **3TI** is nearly planar with efficient π-conjugation and which is the reason for efficient ICT transition from oligothiophene moiety to 1,3-indenedione-vinyl group. Upon interaction with CN^-, the geometry of the sensor molecule changes to the twisted form with a dihedral angle of 47.86° between the oligothiophene and 1,3-indenedione-vinyl groups and as a result π-conjugation breakdown, leads to decrease ICT effects. The interruption of the π-conjugation caused a significant blue shift in fluorescence emission spectra and effectively decreased the ICT character. These DFT results clearly revealed the nucleophilic addition of CN^- to the β-position of C=C and conversation of sp^2 hybridized carbon to sp^3 hybridization.

Detailed information about the noted absorption in the blue shift upon the addition of CN^- with **3TI** can also be gained TD-DFT calculations. As shown in Fig. 8, the calculated absorption wavelengths of **3TI** and **3TI-CN⁻** were 495 nm and 386 nm, respectively, which is in good agreement with the experimental results. Moreover, the HOMO-LUMO energy gap is significantly increased in **3TI-CN⁻** adduct (3.21 eV) compared to **3TI** (2.64 eV), which is well reflected in the changes in UV–vis spectra. Therefore, the DFT and TD-DFT calculations provide reasonable explanations for their electronic structure and optical spectra.

3.6. Response time and effect of pH

To exploit its sensing behavior, we examined the time dependent changes in the fluorescence spectra of **3TI** (1.0 μM) upon reaction with CN^- (10 equiv.) at room temperature. Reaction-based sensors generally suffer from a long response time. As well known, a long response time is

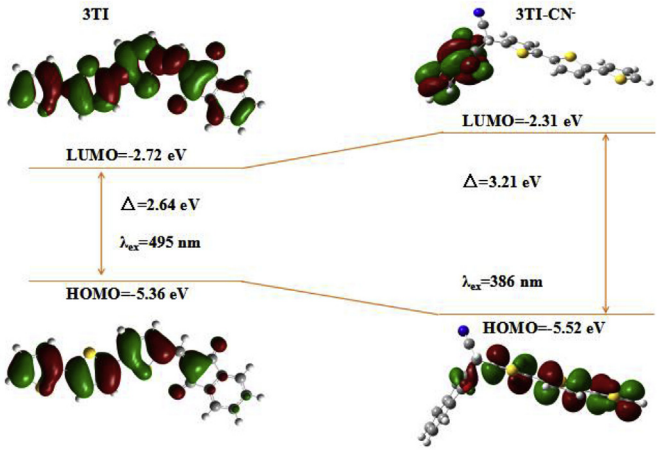

Fig. 8. Frontier molecular orbitals of **3TI** and **3TI-CN⁻**.

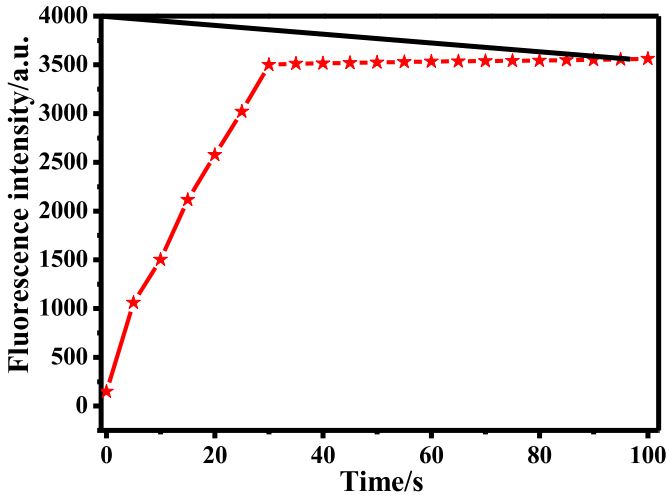

Fig. 9. The pH dependence of the fluorescence intensity of **3TI** at 588 nm with and without CN^- (10.0 equiv.).

a serious problem that sensors often encounter. In our study, the response of **3TI** towards CN^- was found to be very fast. The fluorescence intensity increased at 588 nm and then reached maximum within 30 s in presence of 10 equiv. of CN^-, indicating that the nucleophilic addition reaction between the vinyl group of sensor **3TI** and CN^- was completed (Fig. 9), denoting the rapid reaction of sensor **3TI** with CN^-. Thus, sensor **3TI** can be used to monitor CN^- in real time.

For potential applicability, the pH dependent emission spectral changes of the sensor **3TI** (1.0 μM) in absence and presence of CN^- (10 equiv.) in THF/H_2O (3/7, v/v) solution were investigated as shown in Fig. 10. In different pH conditions (1–14), the fluorescence intensity of the sensor **3TI** is almost unaffected in absence of CN^-. In presence of CN^-, there is a significant enhancement of fluorescence intensity at a range of pH values from 5 to 12. The results indicate that **3TI** can successfully react with CN^- and allow CN^- detection over a wide pH range (5–12), and functions properly at physiological pH.

3.7. Practical applications

Since **3TI** features excellent selectivity, high sensitivity, naked-eye colorimertic and fluorogenic dual responses, instant response time, and excellent anti-interference ability for CN^- in favorable working pH range, it is quite possible to explore its practical applications.

Firstly, we set out to investigate the recognition of CN^- by **3TI**

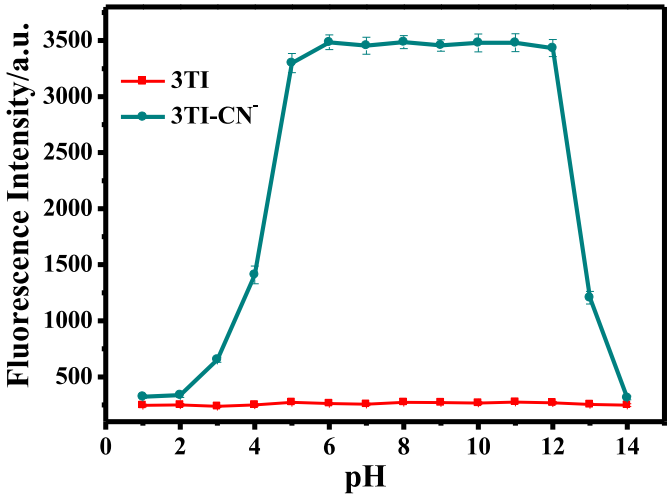

Fig. 10. The response time of sensor **3TI** for CN^-.

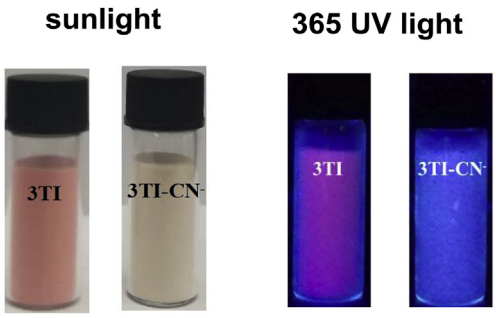

Fig. 11. Color change of silica containing sensor **3TI** for CN^- detection under ambient and 365 nm UV light. (For interpretation of the references to color in this figure legend, the reader is referred to the Web version of this article.)

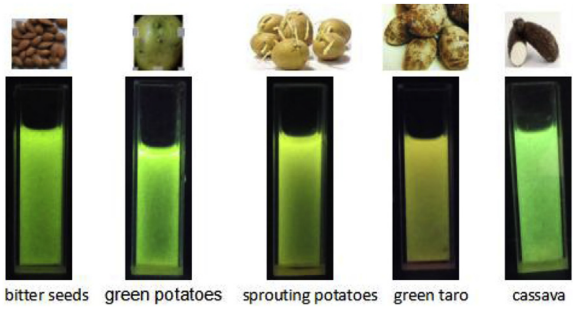

Fig. 12. Solution color changes under 365 nm UV lamp of sensor **3TI** to monitor cyanide in food samples. (For interpretation of the references to color in this figure legend, the reader is referred to the Web version of this article.)

while supported on silica [44]. A solution of **3TI** in THF (1 mL, 10 μM) was added to silica (200–300 mesh, 2 g, colorless), stirred for 1 min, and then the solvent was removed to gain the pink silica (Fig. 11). The pink silica was treated with a solution of CN^- (10 μL, 1.0 mM) in deionized water. An instant color change from pink to colorless in the case of CN^- was noticed. The solvent was removed under reduced pressure, and the silica sample was dried in an oven to obtain the expected material. Since the color change from the pink to colorless was rapidly and clearly detected, sensor **3TI** has the great potential for use in practical application served as an optical solid sensor [45].

Subsequently, the sensor **3TI** was used to detect CN^- in real environmental water samples. Sensor **3TI** sensitivity to CN^- detection in real water samples such as tap water, distilled water, and lake water from Jinan Garden Expo was evaluated by standard addition method. The analytical results were summarized in Table 1. The sensor **3TI** was able to detect the spiked CN^- with good recovery ranged from 98.9% to 100.3% and low relative standard deviation (RSD) below 0.9%, indicating the feasibility and reliability of the sensor for determination of CN^- in environmental water samples. These results ulteriorly proved that **3TI** could act as a potential, simple, effective and convenient fluorescent sensor to detect CN^- in real samples with satisfactory and acceptable results.

Moreover, to further evaluate the practical application of **3TI** for detecting CN^- in human life, the cassava, bitter seeds, green taroes, sprouting and green potatoes were utilized by infusing these food samples in aqueous sodium hydroxide and then filtrating and centrifuging them to obtain the target cyanide-containing solutions. The addition of 1.0 equiv. of each filtrate to the sensor **3TI** (1.0 μM), which gives green color and is similar to that of CN^- anion complex of 3TI (Fig. 12). The qualitative estimation of CN^- from real food samples by using the colorimetric anion sensor **3TI** is an interesting and easy process, which gives rapid response through the naked-eye identification.

Furthermore, fluorescent dyes in cellular biology have become one of the most popular methods for biological analysis since it is a non-destructive way of tracking and analyzing biological molecules [46]. Therefore, to evaluate potential biological applications, the sensor **3TI** as a fluorescent dye for the detection of CN^- in living cells was tested. The cytotoxicity of sensor **3TI** was measured by MTT assay with increasing sensor concentration (Fig. S7). The investigated results indicated that the sensor **3TI** exhibited low cytotoxicity to living cells. Then HeLa cells were chosen as a representative cell line and fluorescent images were recorded under fluorescence microscope. Initially, the incubation of HeLa cells with **3TI** caused almost no fluorescence emission under green field (Fig. 13a and b). Afterwards, a time-course experiment was carried out to monitor the binding process of sensor **3TI** to determine intracellular CN^-. When CN^- was added to HeLa cells and further incubated with sensor **3TI** for 30 min, a green fluorescence was clearly observed (Fig. 13c). As the incubation time was prolonged to 60 min, a bright green fluorescence was identified in the cytoplasm

Table 1
Measurement results of CN^- in environmental water samples.

Sample	Added ($\times 10^7$ M)	Found($x^a \pm$ SD[b]) ($\times 10^7$ M)	Recovery (%)	Relative error (%)	RSD (%)
Distilled	–[c]	–	–	–	–
Water	10	9.98 ± 0.09	99.8	0.2	0.9
	15	15.04 ± 0.12	100.3	0.27	0.79
	20	19.97 ± 0.06	99.9	0.1	0.3
River	–	–	–	–	–
Water	10	9.94 ± 0.07	99.4	0.56	0.71
	15	14.93 ± 0.08	99.5	0.47	0.54
	20	19.79 ± 0.06	98.9	1.05	0.3
Tap	–	–	–	–	–
Water	10	9.97 ± 0.03	99.7	0.3	0.3
	15	14.95 ± 0.06	99.6	0.33	0.4
	20	19.88 ± 0.13	99.4	0.6	0.65
Lake	–	–	–	–	–
Water	10	9.96 ± 0.06	99.6	0.4	0.6
	15	14.85 ± 0.12	99	1	0.81
	20	19.83 ± 0.07	99.1	0.85	0.35

[a] Mean of three determination.
[b] SD: Standard Deviation.
[c] -:No substance added.

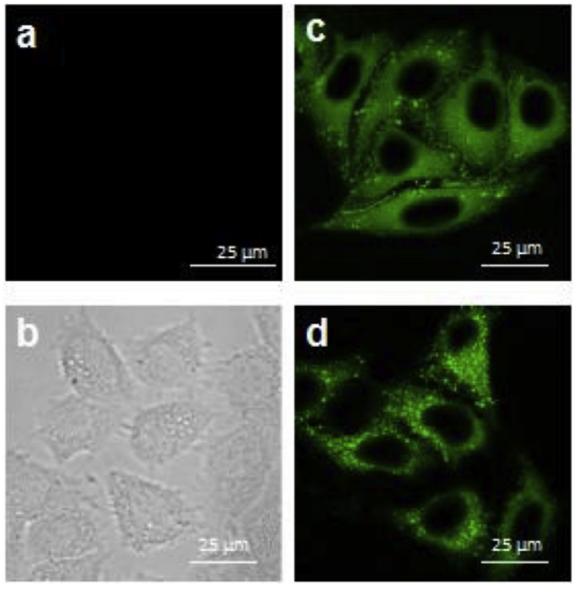

Fig. 13. Confocal microscopy images of HeLa cells. **(a)** Fluorescent images of HeLa cells with **3TI** for 1 h; **(b)** Bright-field image; **(c)** Fluorescent images of HeLa cells incubated with **3TI** and CN^- for 30 min; **(d)** for 60 min.

(Fig. 13d), implying that **3TI** has a very good performance for CN^- imaging in HeLa cells. These cell imaging results suggest that this simple sensor **3TI** can be used for fluorescence imaging of CN^- selectively and sensitively in living cells.

Compared to other CN^--selective sensors (Table S1) [47–52], our designed sensor possessed multiple attractive features including colorimertic and turn-on fluorescent dual-mode detection, excellent anti-interference ability, low detection limit, naked-eye observed color changes, obvious optical spectra changes, fast response time, favorable working pH range, good validity for signaling CN^- on silica and in real water and food samples analysis, good cell membrane permeability and low cytotoxicity for imaging CN^- in living cells.

4. Conclusions

In summary, we reported a new oligothiophene-indenedione-based colorimetric and fluorescent turn-on sensor **3TI** for rapid naked-eye detection of CN^- anions in 70% aqueous solution with excellent overall performance, such as naked-eye observed color changes, remarkable fluorescence enhancement, simple procedure, high sensitivity, excellent anti-interference ability, rapid response, favorable working pH span, and good validity for signaling CN^- on silica and in real water and food samples. Moreover, the detection mechanism was a nucleophilic addition reaction between the sensor **3TI** and CN^-, which inhibited the ICT process as confirmed by optical analysis, ^1H NMR titration, and FTIR spectra, HR ESI-MS analysis as well as the TD/DFT studies. Benefiting from the good water-solubility and good biocompatibility of the **3TI**, this sensor can be applied for subcellular imaging of CN^- in living cells with good cell membrane permeability and low cytotoxicity.

Acknowledgments

We are thankful for the financial support from the National Natural Science Foundation of China (Nos. 21376125, 21776143, and 51702178), the Natural Science Foundation of Shandong Province (No. ZR2017LB009), the program for National College Students' Innovation and Entrepreneurship Training (No. 201710431027), and the Program for Scientific Research Innovation Team in Colleges and Universities of Shandong Province.

Appendix A. Supplementary data

Supplementary data to this article can be found online at https://doi.org/10.1016/j.dyepig.2018.12.057.

References

[1] Vennesland B, Conn EE, Knownles CJ, Westly J, Wissing F. Cyanide in biology. London: Academic Press; 1981.
[2] Young CA, Twidwell LG, Anderson CG, Minerals M, Staff MS, Minerals M, Meeting MS. Cyanide: social, industrial, and economic aspects, TMS (the minerals. Metals & Materials Society); 2001.
[3] Bolarinwa IF, Orfila C, Morgan MRA. Determination of amygdalin in appleseeds, fresh apples and processed apple juices. Food Chem 2015;170:437–42.
[4] Miller GC, Pritsos CA. Cyanide: soc., Ind. Econ. Aspects. Proc Symp Appl Math 2001:73–81.
[5] Kaim W, Schwederski B, Klein A. Bioinorganic chemistry – inorganic elements in the chemistry of life: an introduction and guide. Wiley; 2013.
[6] WHO guidelines for drinking-water quality: recommendations. World Health Organization; 2004.
[7] Guidelines for drinking-water quality. Geneva: World Health Organization; 1996.
[8] Sun Y, Zhao H, Boussouar I, Zhang F, Tian D, Li H. Highly sensitive chiral sensing by calix[4]arene-modified silvernanoparticles via dynamic light scattering. Sens Actuators B 2015;216:235–9.
[9] Sun Y, Ma J, Tian D, Li H. Macroscopic switches constructed through host-guest chemistry. Chem Commun 2016;52:4602–12.
[10] Zhou X, Kim J, Liu Z, Jo S, Pak YL, Swamy KMK. Selective fluorescent and colorimetric recognition of cyanide via altering hydrogen bonding interaction in aqueous solution and its application in bioimaging. Dyes pigm 2016;128:256–62.
[11] Xu Z, Chen X, Kim HN, Yoon J. Sensors for the optical detection of cyanide ion. Chem Soc Rev 2010;39:127–37.
[12] Lou X, Ou D, Li Q, Li Z. An indirect approach for anion detection: the displacement strategy and its application. Chem Commun 2012;48:8462–77.
[13] Yang Y, Zhao Q, Feng W, Li FY. Luminescent chemodosimeters for bioimaging. Chem Rev 2013;113:192–270.
[14] Niu Q, Sun T, Li T, Guo Z, Pang H. Highly sensitive and selective colorimetric/fluorescent probe with aggregation induced emission characteristics for multiple targets of copper, zinc and cyanide ions sensing and its practical application in water and food samples. Sens Actuators B 2018;266:730–43.
[15] Peng M, Guo Y, Yang X, Wang L, An J. A highly selective ratiometric and colorimetric chemosensor for cyanide detection. Dyes Pigments 2013;98:327–32.
[16] Sun Y, Wang G, Guo W. Colorimetric detection of cyanide with N-nitrophenylbenzamide derivatives. Tetrahedron 2009;65:3480–5.
[17] Wang F, Wang L, Chen X, Yoon J. Recent progress in the development of fluorometric and colorimetric chemosensors for detection of cyanide ions. Chem Soc Rev 2014;43:4312–24.
[18] Hong SJ, Yoo J, Kim SH, Yoon J, Lee CH. Beta-vinyl substituted calix[4]pyrrole as a selective ratiometric sensor for cyanide anion. Chem Commun (J Chem Soc Sect D) 2009;2:189–91.
[19] Yang L, Li X, Yang J, Qu Y, Hua J. Colorimetric and ratiometric near-infrared fluorescent cyanide chemodosimeter based on phenazine derivatives. ACS Appl Mater Interfaces 2013;5:1317–26.
[20] Lee CH, Yoon HJ, Shim JS, Jang WD. boradiazaindacene-based turn-on fluorescent probe for cyanide detection in aqueous media. Chem Eur J 2012;18:4513–6.
[21] Liu Z, Wang X, Yang Z, He W. Rational design of a dual chemosensor for cyanide anion sensing based on dicyanovinyl-substituted benzofurazan. J Org Chem 2011;76:10286–90.
[22] Niu Q, Lan L, Li T, Guo Z, Jiang T, Zhao Z, Feng Z, Xi J. A highly selective turn-on fluorescent and naked-eye colorimetric sensor for cyanide detection in food samples and its application in imaging of living cells. Sens Actuators B 2018;276:13–22.
[23] Lan L, Li T, Wei T, Pang H, Sun T, Wang E, Liu H, Niu Q. Oligothiophene-based colorimetric and ratiometric fluorescence dual-channel cyanide chemosensor: sensing ability, TD-DFT calculations and its application as an efficient solid state sensor. Spectrochim Acta A 2018;193:289–96.
[24] Bera MK, Chakraborty C, Singh PK, Sahu C, Sen K, Maji S, Das AK, Malik S. Fluorene-based chemodosimeter for "turn-on" sensing of cyanide by hampering ESIPT and live cell imaging. J Mater Chem B 2014;2:4733–9.
[25] Dvivedi A, Rajakannu P, Ravikanth M. meso-Salicylaldehyde substituted BODIPY as a chemodosimetric sensor for cyanide anions. Dalton Trans 2015;44:4054–62.
[26] Niamnont N, Khumsri A, Promchat A, Tumcharern G, Sukwattanasinitt M. Novel salicylaldehyde derivatives as fluorescence turn-on sensors for cyanide ion. J Hazard Mater 2014;280:458–63.
[27] Pati PB, Zade SS. Selective colorimetric and "Turn-on" fluorimetric detection of cyanide using a chemodosimeter comprising salicylaldehyde and triphenylamine groups. Eur J Org Chem 2012;33:6555–61.
[28] Huang X, Gu X, Zhang G, Zhang D. A highly selective fluorescence turn-on detection of cyanide based on the aggregation of tetraphenylethylene molecules induced by chemical reaction. Chem Commun (J Chem Soc Sect D) 2012;48:12195–7.
[29] Shankar BH, Jayaram DT, Ramaiah D. A reversible dual mode chemodosimeter for the detection of cyanide ions in natural sources. Chem Asian J 2014;9:1636–42.
[30] Shiraishi Y, Nakamura M, Yamamoto K, Hirai T. Rapid, selective, and sensitive fluorometric detection of cyanide anions in aqueous media by cyanine dyes with indolium–coumarin linkages. Chem Commun (J Chem Soc Sect D) 2014;78:11583–6.
[31] Wang S, Xu H, Yang Q, Song Y, Li Y. A triphenylamine-based colorimetric and "turn-on" fluorescent probe for detection of cyanide anions in live cells. RSC Adv 2015;59:47990–6.
[32] Sun T, Niu Q, Li Y, Li T, Hu T, Wang E, Liu H. A novel oligothiophene-based colorimetric and fluorescent "turn on" sensor for highly selective and sensitive detection of cyanide in aqueous media and its practical applications in water and food samples. Sens Actuators B 2018;258:64–71.
[33] Pramanik S, Bhalla V, Kumar M. Hexaphenylbenzene-based fluorescent aggregates for ratiometric detection of cyanide ions at nanomolar level: set–reset memorized sequential logic device. ACS Appl Mater Interfaces 2014;6:5930–9.
[34] Cheng J, Liang X, Cao Y, Guo K, Wong WY. Aldehyde end-capped terthiophene with aggregation-induced emission characteristics. Tetrahedron 2015;71:5634–9.
[35] Frisch MJ, Trucks GW, Schlegel HB, Scuseria GE, Robb MA, Cheeseman JR, Scalmani G, Barone V, Mennucci B, Petersson GA. Gaussian 09, revision A.2. Wallingford CT: Gaussian, Inc.; 2009.
[36] Becke AD. Density-functional thermochemistry. III. The role of exact exchange. J Chem Phys 1993;98:5648–52.
[37] Hehre WJ, Ditchfield R, Pople JA. Self-consistent molecular orbital methods. XII. Further extensions of Gaussian-type basis sets for use in molecular orbital studies of organic molecules. J Chem Phys 1972;56:2257–61.
[38] Jo TG, Na YJ, Lee JJ. A multifunctional colorimetric chemosensor for cyanide and copper(II) ions. Sens Actuators B 2015;211:498–506.
[39] Yoo M, Park S, Kim HJ. Highly selective detection of cyanide by 2-hydroxyphenylsalicylimine of latent fluorescence through the cyanide-catalyzed imine–-to–oxazole transformation. Sens Actuators B 2015;220:788–93.
[40] Table of regulated drinking water contaminants Washington, DC, USA https://www.epa.gov/ground-water-and-drinkingwater/table-regulated-drinking-water-contaminants.
[41] Cheng XH, Tang RL, Jia HZ, Feng J, Qin JG, Li Z. New fluorescent and colorimetric probe for cyanide: direct reactivity, high selectivity, and bioimaging application. Appl. Mater. Interfaces. 2012;4:4387–92.
[42] Yang L, Li X, Yang JB, Qu Y, Hua JL. Colorimetric and ratiometric Near-Infrared fluorescent cyanide chemodosimeter based on phenazine derivatives. Appl. Mater.

Interfaces. 2013;5:1317–26.
[43] Fillaut J-L, Akdas-Kilig H, Dean E, Latouche C, Boucekkine A. Switching of reverse charge transfers for a rational design of an OFF-ON phosphorescent chemodosimeter of cyanide anions. Inorg Chem 2013;52:4890–7.
[44] Jo TG, Na YJ, Lee JJ. A multifunctional colorimetric chemosensor for cyanide and copper(II) ions. Sens Actuators B 2015;211:498–506.
[45] Yoo M, Park S, Kim HJ. Highly selective detection of cyanide by 2-hydroxyphenylsalicylimine of latent fluorescence through the cyanide-catalyzed imine–-to–oxazole transformation. Sens Actuators B 2015;220:788–93.
[46] Yang Y, Zhao Q, Feng W, Li F. Luminescent chemodosimeters for bioimaging. Chem Rev 2013;113:192–270.
[47] Li Z, Liu C, Wang S, Xiao L, Jing X. Visual detection of cyanide ion in aqueous medium by a new chromogenic azo-azomethine chemosensor. Spectrochim Acta A 2019;210:321–8.
[48] Chemchem M, Yahaya I, Aydiner B, Seferoğlu N, Doluca O, Merabet N, Seferoğlu Z. A novel and synthetically facile coumarin-thiophene-derived Schiff base for selective fluorescent detection of cyanide anions in aqueous solution: synthesis, anion interactions, theoretical study and DNA-binding properties. Tetrahedron 2018;74:6897–906.
[49] Long C, Hu J-H, Ni P-W, Yin Z, Fu Q-Q. A novel colorimetric and ratiometric fluorescent CN^- sensor based on rhodamine B hydrazone derivatives in aqueous media and its application in sprouting potatoes. New J Chem 2018;42:17056–61.
[50] Orojloo M, Amani S. Naked-eye detection of cyanide ions in aqueous media based on an azo-azomethine chemosensor. C. R. CHIM. 2017;20:415–23.
[51] Thanayupong E, Suttisintong K, Sukwattanasinitt M, Niamnont N. Turn-on fluorescent sensor for the detection of cyanide based on a novel dicyanovinyl phenylacetylene. New J Chem 2017;41:4058–64.
[52] Sun Y, Hu J-H, Qi J, Li J-B. A highly selective colorimetric and “turn-on” fluorimetric chemosensor for detecting CN^- based on unsymmetrical azine derivatives in aqueous media. Spectrochim Acta A 2016;167:101–5.